

# UNCERTAINTY QUANTIFICATION OF NOISE ABATEMENT FLIGHT PROCEDURES

W.F.J. Olsman

*DLR in der Helmholtz-Gemeinschaft  
Institute of Aerodynamics and Flow Technology, Helicopter Division  
Lilienthalplatz 7, 38108 Braunschweig, Germany*

## Abstract

Noise abatement flight procedures are usually designed under the assumption that the resulting flight path will be executed by the pilot with very high accuracy. A previous investigation, however, has shown that even though the flight path is accurately controlled there still is a significant spread in the measured noise metric on the ground. The statistical values obtained in these flight tests are used in this paper to investigate the influence of uncertainty in the position, velocity and wind. The results indicate that the velocity along the flight path plays a dominant role in the resulting statistical properties of the noise metric on the ground. Furthermore it is shown that uncertainty in the velocity has a significant impact on benefit obtained by noise abatement flight procedures. This indicates the need to include uncertainty into the optimisation process. The results of the uncertainty quantification could also be used to compare different flight procedures in terms of robustness.

## 1 INTRODUCTION

Demands from the public to lower helicopter noise and demands for increased operations while keeping the noise within limits are the main drivers for research into helicopter noise. There are different approaches to minimise the noise of helicopters, either by improved design or by operational restrictions. Noise abatement flight procedures fall into the last category. By changing the flight path the noise is redistributed away from noise sensitive areas and/or minimised by avoiding noisy flight conditions. The advantage of noise abatement flight procedures over newly designed helicopters, is that they can be implemented quickly and can be applied to the current helicopter fleet, while newly designed helicopters will take years to replace the current fleet.

Within CleanSky the subproject GreenRotorcraft 5 is devoted to the minimisation of rotorcraft noise by the use of environmentally friendly flight procedures. New procedures are usually designed based on numerical prediction codes, such as SELENE<sup>5</sup> or HELENA<sup>4</sup>. These codes

compute the noise footprint of a flight procedure based on a number of input parameters, such as the flight path, the take-off weight, wind direction, etc. However, in practice many of the input parameters are not known exactly. For instance the wind magnitude and direction typically vary from day to day in real world applications. Such input parameters are therefore better described by a probability distribution with given properties, such as mean, standard deviation, etc. Similarly the optimised flight path will in practice be flown with a finite accuracy, which depends on the procedure, the guidance system used, weather conditions and pilot skill. A recent experimental study has shown that significant variations in measured noise occur, even though the flight path is accurately controlled<sup>7</sup>. This stresses the importance of obtaining and evaluating statistical information about the noise emissions and the flight path.

Furthermore it is desirable to design flight procedures in such a way that the noise benefit is not compromised by small changes in wind magnitude/direction or flight path, i.e. the flight procedure should be robust.

In the current investigation DLR's noise prediction tool chain SELENE is used to investigate the influence of uncertainties in the flight path and weather conditions. This is widely known as Uncertainty Quantification (UQ). A straightforward method for such an UQ is the Monte Carlo method<sup>9</sup>, however, the computational demands become intractable. Alternatively a Polynomial Chaos Expansion (PCE) can be computed<sup>3</sup>. In the current investigation the non-intrusive PCE method, implemented in the open source software DAKOTA<sup>1</sup>, is used.

Most of the prediction codes use a database for the noise source description (noise hemisphere database). This database can be based on flight experiments or on numerical computations. Such a database contains uncertainty due to inaccuracies in the numerical modeling or due to measurement uncertainties. The hemisphere database used in the current investigation is based on dedicated flight tests<sup>10</sup>. Even though these experiments are carried out with great care and accuracy, there still remains an uncertainty in the measurements. Each point on each noise hemisphere will therefore have statistical properties. In order to obtain an estimate of these properties the flight procedures for specific flight conditions need to be executed multiple times, which will require a significant amount of flight hours. The resulting uncertainty quantification computation can easily lead to the use of thousands of random variables, which will induce high computational cost for solving the problem. The use of uncertainty in the aeroacoustic database is therefore outside the scope of the current investigation and the experimental database is used as is.

This paper is organised as follows. First a short overview of possible methods for uncertainty quantification are presented in section 2. Then in section 3 the uncertainty quantification method is applied to a standard approach procedure, for which experimental data is available, and subsequently to more practically relevant three-dimensional procedures. Lastly in section 4 the conclusions are presented.

## 2 UNCERTAINTY QUANTIFICATION

The problem of computing how uncertainty in the input of a model is propagating through the model

is generally known as Uncertainty Quantification (UQ). In the current investigation the model consists of the complete noise footprint prediction tool chain SELENE, together with the experimental database of noise sources.

### 2.1 Monte Carlo simulation

A straightforward approach to UQ is the application of the Monte Carlo (MC) method<sup>9</sup>. With this method a statistical distribution is assumed for the input variable(s) of the model and a large number of possible values for the input variable(s) are used to compute the corresponding output. From the output samples the statistical properties of the output can be estimated. The main drawback of this method lies in the large number of samples that is needed for a reliable estimation of the statistical properties. The number of samples grows exponentially with the number of uncertain input variables (if the number of samples in each dimension is the same) which quickly leads to impractical computational resource requirements.

However, if a simple surrogate model of the original (complex) model can be derived. Then this surrogate model can be used for Monte Carlo simulation. Since no simple (quick to evaluate) surrogate model is available for the acoustical computational chain the use of the Monte Carlo method is currently not practically possible and is only used in a one-dimensional case for verification purposes.

### 2.2 Polynomial Chaos Expansion

An alternative for the Monte Carlo method is Polynomial Chaos Expansion (PCE)<sup>11;12</sup>. The general idea in PCE is to build a surrogate model that models the statistical properties of the original model. Note that this is different from the usual surrogate models that are built to represent the outcome of the model. In the PCE it is in theory not relevant what the outcome of the surrogate model is, as long as the statistical properties are the same as that of the original model. It may seem tempting to use the PCE as a surrogate model for the output of the original model, however, one should keep in mind that this has no theoretical foundation. The uncertainty quantification based on PCE can also be implemented

in the optimization procedure, such as described in<sup>6</sup>. This is, however, outside the scope of the current investigation.

Below follows a short description of the polynomial chaos expansion method. Assume a model  $f$  with input  $x$  and output  $y$ , such that  $f(x) = y$ . Now assume that the input is uncertain and described by a statistical distribution  $X$ , correspondingly the output has distribution  $Y$ . The problem is then: given the statistical properties of  $X$  compute that of  $Y$ . In PCE  $Y$  is modelled by a polynomial expansion

$$(1) \quad Y = f(X) = \sum_{i=0}^{\infty} a_i \Psi_i(X),$$

with  $\Psi_i$  orthogonal polynomials and  $a_i$  coefficients. If the model has a single input but multiple output the coefficients  $a_i$  are vectors. In practice the infinite sum in equation 1 needs to be terminated at a finite number of terms. The procedure to determine how many terms are needed is rather add hoc. It is hoped that with more terms the coefficients become smaller, such that the series converges. Since the number of terms in equation 1 is directly related to the highest power of the polynomial in the expansion, the number of terms is also referred to as the order of the PCE.

In order to determine the values of the coefficients  $a_i$  in equation 1 an inner product is defined as

$$(2) \quad \langle g_1, g_2 \rangle = \int g_1(\xi) g_2(\xi) w(\xi) d\xi.$$

Here  $w$  is a weighting function that is equal to the probability density function of the input distribution (see table 1). The coefficients  $a_i$  can then be computed from a Galerkin projection. Here the orthogonality of the polynomials is exploited.

$$(3) \quad a_i = \frac{\langle f(X), \Psi_i \rangle}{\langle \Psi_i, \Psi_i \rangle}$$

In general the value of the inner product  $\langle \Psi_i, \Psi_i \rangle$  is known analytically. The integral in the numerator of equation 3 is in general evaluated numerically. For the numerical integration of the numerator evaluations of the original model are needed.

Alternatively to the Galerkin projection the collocation method can be used. Here the finite sum is evaluated at a fixed number of points and the

output is equated to the corresponding output of the original model. This leads to a square matrix system that can be solved for the values of the coefficients.

The polynomials  $\Psi$  and the weighting function  $w$  are chosen based on the distribution of the input  $X$ . The polynomials and corresponding weighting function are shown in table 1 for different distributions.

It is assumed here the expansion is terminated after  $N$  terms. Once the coefficients are known the moments of the distribution can be computed. The expected value  $E$  is given by

$$(4) \quad E[Y] = \int \left( \sum_{i=0}^N a_i \Psi_i(\xi) \right) \rho(\xi) d\xi = a_0.$$

Where  $\rho$  is the probability density function for the corresponding distribution (see table 1). The integral is to be taken over the support range of the distribution. Note that including more terms in the expansion does not affect the mean value of the PCE. The approximation of the mean can only be improved by increasing the accuracy of the approximation of the integral in the numerator of equation 3, for instance by including more quadrature points or using a different quadrature rule. The variance is computed as

$$(5) \quad \text{Var}(Y) = E[Y^2] - (E[Y])^2 = \int \left( \sum_{i=0}^N a_i \Psi_i(\xi) - a_0 \right)^2 \rho(\xi) d\xi = \sum_{i=1}^N a_i^2.$$

Similarly higher order moments of the distribution can be computed. The probability density function (PDF) can be estimated by the use of Monte Carlo sampling, since the evaluation of the PCE is cheap. The PDF can be estimated by a histogram or alternatively by Kernel Density Estimation. In addition to the PDF the moments of the distribution can be estimated from the Monte Carlo samples as well.

The procedure described above can also be extended to multiple dimensions. In this case the input  $x$  is a vector  $\vec{x}$  and as before the output can also be a vector  $\vec{y}$ . In this case the coefficients  $a_i$  are vectors and the polynomials  $\Psi$  are replaced by a products of polynomials

$$(6) \quad \Theta_i(\vec{X}) = \prod_{j=0}^M \Psi_j(X_j),$$

Distribution	Probability density function	Polynomial	Weight function	Support range
Normal	$\frac{1}{\sqrt{2\pi}} e^{-\frac{x^2}{2}}$	Hermite	$e^{-\frac{x^2}{2}}$	$[-\infty, \infty]$
Uniform	$\frac{1}{2}$	Legendre	1	$[-1, 1]$
Beta	$\frac{(1-x)^\alpha(1+x)^\beta}{2^{\alpha+\beta+1}B(\alpha+1,\beta+1)}$	Jacobi	$(1-x)^\alpha(1+x)^\beta$	$[-1, 1]$
Exponential	$e^{-x}$	Laguerre	$e^{-x}$	$[0, \infty]$
Gamma	$\frac{x^\alpha e^{-x}}{\Gamma(\alpha+1)}$	Generalized Laguerre	$x^\alpha e^{-x}$	$[0, \infty]$

Table 1: Linkage between standard distributions and corresponding Askey polynomials, from<sup>3</sup>.

where  $M$  corresponds to the number of uncertain variables (or the dimension). The Galerkin projection to evaluate the coefficients of the expansion now results in a multidimensional integral.

As with Monte Carlo simulation the number of function evaluations grows exponentially with the number of uncertain variables (the number of dimensions). The advantage lies in the fact that the base of the exponent is significantly lower with PCE.

There are two approaches to implement PCE, either intrusive or non-intrusive. In the intrusive method the approach is directly implemented in the numerical code. This has the advantage that a high computational efficiency can be achieved, however, the implementation is more difficult. In the non-intrusive implementation the method uses a given simulation code as a blackbox. This means that the simulation code needs only minimal (or no) modifications at the cost of less computational efficiency.

For the current study the implementation of the non-intrusive PCE, available in the open source software DAKOTA<sup>1</sup>, is chosen.

The DAKOTA software is coupled with the computational chain SELENE. SELENE stands for Sound Exposure Level starting from Evaluation of Noise Emissions. It is a computational chain for helicopter flyover noise prediction. The chain consists of a flight path generator, a flight mechanical code, a noise propagation code and an aeroacoustic database for the noise source description. The flight path generator computes the flight path based on user provided control points. Then a time accurate simulation with the flight mechanical code HOST<sup>2</sup> is used to obtain the flight mechanical parameters along the flight path. According to the tip path plane angle of attack, the advance ratio and the thrust coefficient

a noise source description is selected from the aeroacoustic database and the noise is propagated to the ground, taking into account spherical spreading, Doppler frequency shift, wind effects, atmospheric absorption and ground reflection. For a more detailed description of the computational method the reader is referred to previous publications<sup>5;8</sup>.

In case of noise prediction of helicopter noise the model  $f$ , in equation 1, represents the complete computational chain SELENE and the input  $x$  consists of the flight path, atmospheric properties, take-off weight of the helicopter, etc.

### 3 RESULTS

In the previous section the polynomial chaos expansion was described as an efficient method for uncertainty quantification. In this section this method is applied to flight procedures in order to assess the robustness of these procedures.

#### 3.1 Two-dimensional reference procedure

As a testcase a two-dimensional reference approach procedure is considered. This procedure is not a noise abatement flight procedure, but represents a standard approach flight procedure for an EC135 helicopter. It was flown extensively with the EC135-ACT/FHS helicopter during previous flight tests<sup>7</sup>. Relevant parameters for this approach procedure are shown in figure 1. Here the red line shows the height as a function of time, the green line shows the velocity in knots and in blue the rate of descent is shown. It should be noted that the number of approaches available (about 25) is far from enough for a reliable estima-

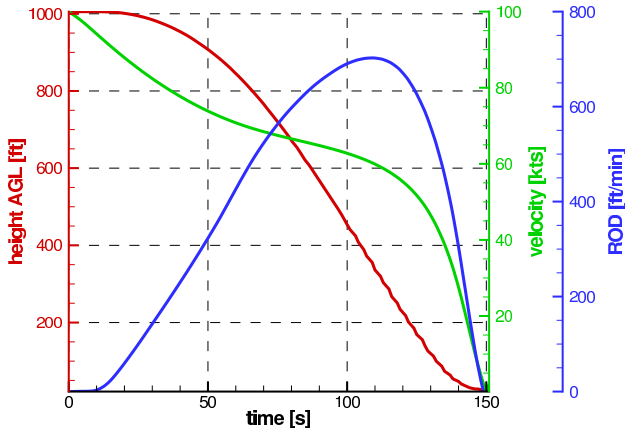


Figure 1: Height above ground level (AGL) in ft, ground velocity in knots and rate of descent (ROD) in ft/min as a function of time for the reference procedure.

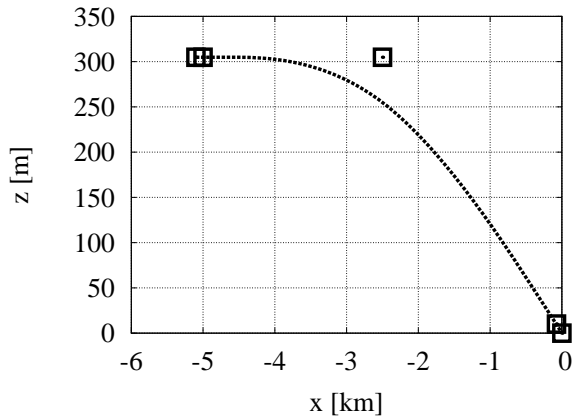


Figure 2: Reference approach procedure in the vertical plane. Control points of the flight path are shown by the square markers.

tion of the probability density functions, nevertheless an estimation was attempted. The number of approaches should, however, be sufficient for reasonable estimates of the means and standard deviations.

The flight path is shown in the vertical plane in figure 2. The five control points that control the Bezier spline that defines the flight path are shown by the square markers. At every control point there are four degrees of freedom, the position  $x$ ,  $y$ ,  $z$  and the magnitude of the velocity  $|\vec{v}|$ . The number of degrees of freedom grows quickly with the number of control points and hence the number of uncertain variables quickly becomes large. The number of output parameters (number of microphones) is not significant in this context,

since the simulation of the flight path and subsequent computation of the noise emission requires much more time than the evaluation of the numerical quadratures in order to obtain the coefficients of the PCE.

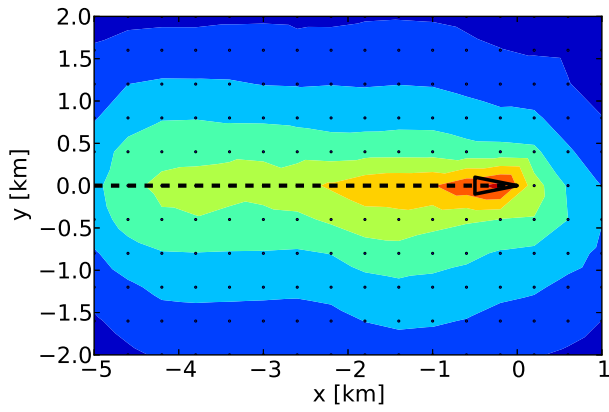
During experiments a slalom behavior in the flight path in the horizontal plane was observed<sup>7</sup>. To model such flight path deviations requires manipulation of many control points. This leads to a high number of uncertain variables which results in an intractable amount of required computational time. Therefore it was chosen to only consider the third control point, located at  $x = -2.5$  km, as an uncertain variable.

### 3.1.1 Velocity uncertainty

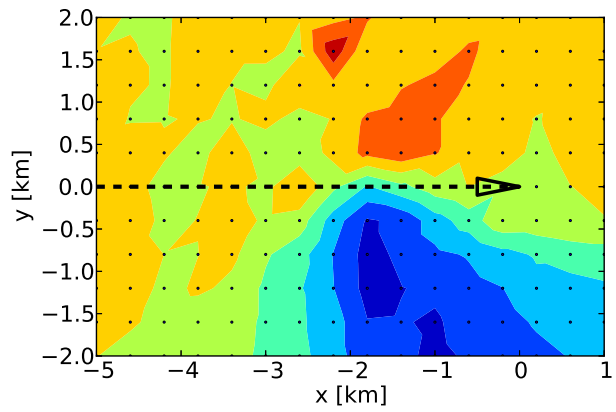
First the velocity magnitude at the control point is considered. Experimental data suggests that the distribution of the velocity is asymmetric and has a standard deviation of 3 m/s. At high velocity the standard deviation tends to be high and the distribution is asymmetric due to the fact that the helicopter is close to its maximum velocity. At intermediate velocity the distribution is likely more symmetric and the standard deviation is lower. At very low velocity the distribution is again asymmetric due to the fact that the magnitude of the velocity cannot be negative.

The velocity at the third control point is modeled by a Beta distribution that has its mode at the initial value of 33.4 m/s, its minimum at 24 m/s, its maximum at 38 m/s and a standard deviation ( $\sigma$ ) of 3 m/s. The values for  $\alpha$  and  $\beta$  are 2.52 and 1.74, correspondingly. Note that the values for  $\alpha$  and  $\beta$  are based on the standard definition of the Beta distribution, which is different from the definition given in table 1. The Beta distribution has a finite range, as opposed to the normal distribution, which has infinite range. This makes the Beta distribution more suitable to model parameters that cannot be negative or cannot exceed a certain limit. The Probability Density Function (PDF) of this distribution is shown in figure 3. Note that the mean value ( $\mu$ ) of 32.3 m/s is to the left of the mode, because the distribution is asymmetric.

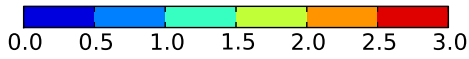
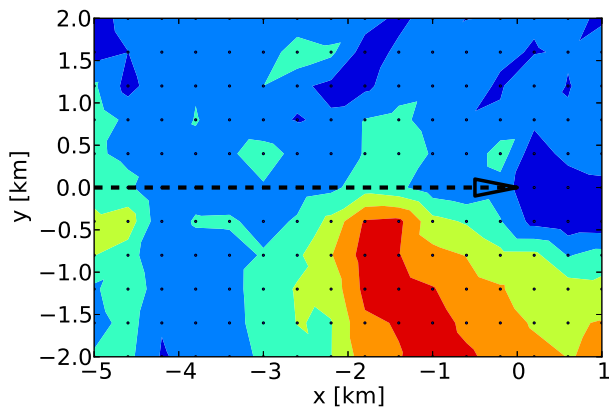
The PCE is computed using a 7th order expansion. The integrals are computed using a standard quadrature. The mean, standard devi-



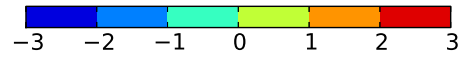
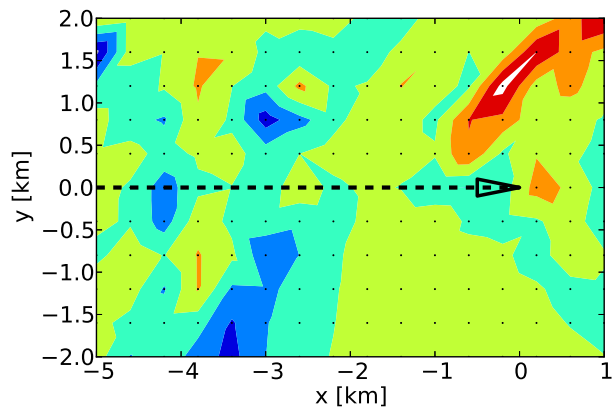
(a) Mean values in dB(A) SEL.



(b) Difference in dB(A) SEL.



(c) Standard deviation in dB(A) SEL.



(d) Skewness in dB(A) SEL.

Figure 4: Mean, mean minus nominal, standard deviation and skewness computed by using a 7th order PCE with the magnitude of the velocity at the third control point as uncertain parameter.

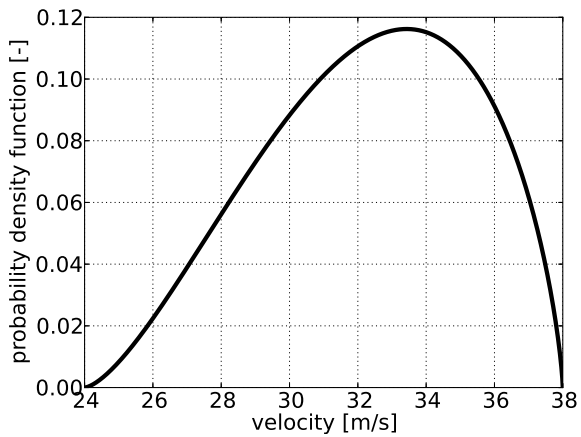


Figure 3: Probability density function of the Beta distribution used to model the magnitude of the velocity at the third control point.

ation and skewness of the Sound Exposure Level (SEL) noise footprint of the flight procedure are shown in figure 4. The microphones are shown by the black dots. The flight path is indicated by the dashed black line and the flight direction is from left to right. The landing point is located at  $(x, y) = (0, 0)$ . Figure 4(a) shows the mean SEL values, the steps between the levels are 5 dB(A). The mean noise footprint is asymmetric, which is expected due to the asymmetric noise radiation of the helicopter. A difference plot where the undisturbed footprint is subtracted from the mean value footprint is shown in figure 4(b). This plot indicates that there is a significant increase in the mean value on the advancing blade side. The standard deviation is shown in figure 4(c) and dis-

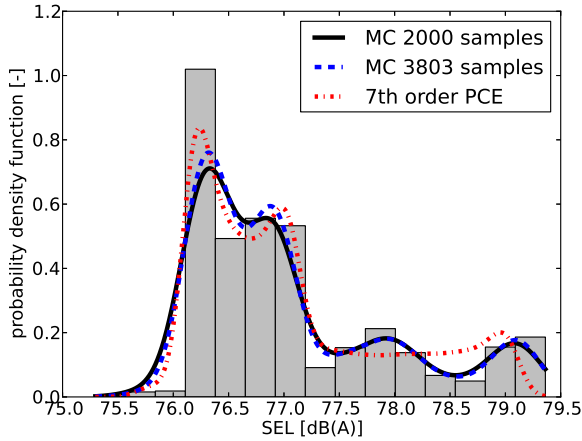


Figure 5: Probability density function of the Sound Exposure Level on the ground, due to uncertainty in the velocity magnitude at one control point.

plays values up to 2.5 dB(A). The highest values occur on the advancing side of the rotor. Most likely due to Blade Vortex Interaction (BVI) noise, which tends to radiate most intense on the advancing blade side. The skewness of the SEL footprint is shown in figure 4(d) and there are regions with positive and regions with negative skewness. In case there is only one maximum in the PDF positive skew means that the PDF of the SEL footprint is asymmetric and its mean is to the right of the mode, whereas negative skew indicates that the mean is to the left of the mode. A further investigation of the PDF at certain microphone locations shows that most PDF's have two or more maxima, such that the interpretation of the skewness plot is not straightforward.

In order to verify that the 7th order expansion is accurate the same computation has been conducted for a 24th order expansion. The results are similar to those shown in figure 4. The maximal difference in mean and standard deviation are 0.22 and 0.28 dB(A), respectively. This indicates that for this case a 7th order expansion is sufficient.

With PCE one hopes that the absolute value of the coefficients becomes smaller for higher order polynomial terms. In case the magnitude of the velocity is considered as uncertain parameter this convergence is not very good. This could be due to the distribution of the SEL values on the ground being very irregular. In order to investi-

gate this further a Monte Carlo simulation is performed with 3803 samples. This MC reveals that the PDF's of the SEL values on the ground have many different shapes, most of them with multiple local maxima. A typical example of a PDF for the SEL value on the ground is shown in figure 5.

The solid line displays the PDF based on the MC simulation with 2000 samples and the dashed line shows the PDF based on the MC simulation with 3803 samples. These lines are obtained by kernel density estimation. The lines are nearly on top of each other, which indicates that enough samples are available for the estimation of the PDF. The gray boxes show a histogram based on the MC results with 3803 samples. The dash-dotted line displays the PDF based on a 7th order PCE. Most of the PDF's display multiple maxima, which is an indication of non-linearity in the model. For estimation of the PDF the PCE may not be suitable, however, for lower order moments of the distribution, such as the mean value and the standard deviation it is sufficient. A plot of the mean, standard deviation and skewness, based on the MC results are nearly identical to those shown in figure 4. The maximal difference in mean and standard deviation are 0.2 and 0.27 dB(A), respectively.

A disadvantage of the PCE is that if an error occurs for a certain evaluation point, needed for the numerical integration, the complete quadrature fails and no results can be obtained. Particularly in multiple dimensions with many evaluation points this becomes an issue. Restarting the evaluation at a different point in the neighborhood of the failed point is in general no solution, since the evaluation points of the numerical quadrature are not arbitrary but are specific for the chosen quadrature rule. With MC simulation failed computations can simply be discarded.

### 3.1.2 Position uncertainties

In the previous section the uncertainty in the velocity has been investigated. In this section the velocity and the  $y$  and  $z$  position of the third control points are considered as uncertain parameters. The values that define the Beta distributions are again based on experimental data and shown in table 2. The PCE is computed by a 7th order expansion. The results are shown in

figure 6. These plots look very similar to those shown in figure 4. This leads to the conclusion that the uncertainty in the velocity dominates the results. A separate computation where the velocity is fixed and only the  $y$  and  $z$  position are considered as uncertain confirms this. For this case with only two uncertain parameters the mean SEL footprint is very similar to that shown in figures 4 and 6. The standard deviation is below 0.6 dB(A) at most locations and at most 1 dB(A) at a very limited number of locations. For this case the convergence of the PCE coefficients is much better compared to the convergence in case of the velocity uncertainty and the PDF's are close to the PDF's of the input in terms of their shape.

The dominant role of the velocity is not unexpected. The velocity evolution along the flight path directly influences the acceleration along it. The acceleration in turn has a direct influence on the tip path plane angle of attack, which is the most dominant parameter controlling BVI noise radiation. Furthermore the velocity also controls the advance ratio, which is the second most significant parameter for controlling BVI noise radiation.

Changes in the  $z$  position change the flight path angle and thereby also the tip path plane angle of attack. However, this influence is small because the deviation in the  $z$  direction are small compared to the range in  $x$  direction.

### 3.1.3 Atmospheric uncertainty

In the previous section the effect of uncertainty in the flight path position and velocity has been investigated. In this section the focus is on atmospheric conditions. The investigation is limited to uncertainty in wind direction and magnitude. Wind has an influence on both the flight mechanics along the flight path and on the propagation of sound through the atmosphere from the source

	Min.	Max.	$\mu$	$\sigma$	$\alpha$	$\beta$
$ \vec{v} $	24.0	38.0	32.3	3.0	2.52	1.74
$y$	-18.0	18.0	0.0	6.0	4.0	4.0
$z$	268.8	340.8	304.8	12.0	4.0	4.0

Table 2: Parameters of the different Beta distributions. Values are in m for the position and m/s for the velocity.

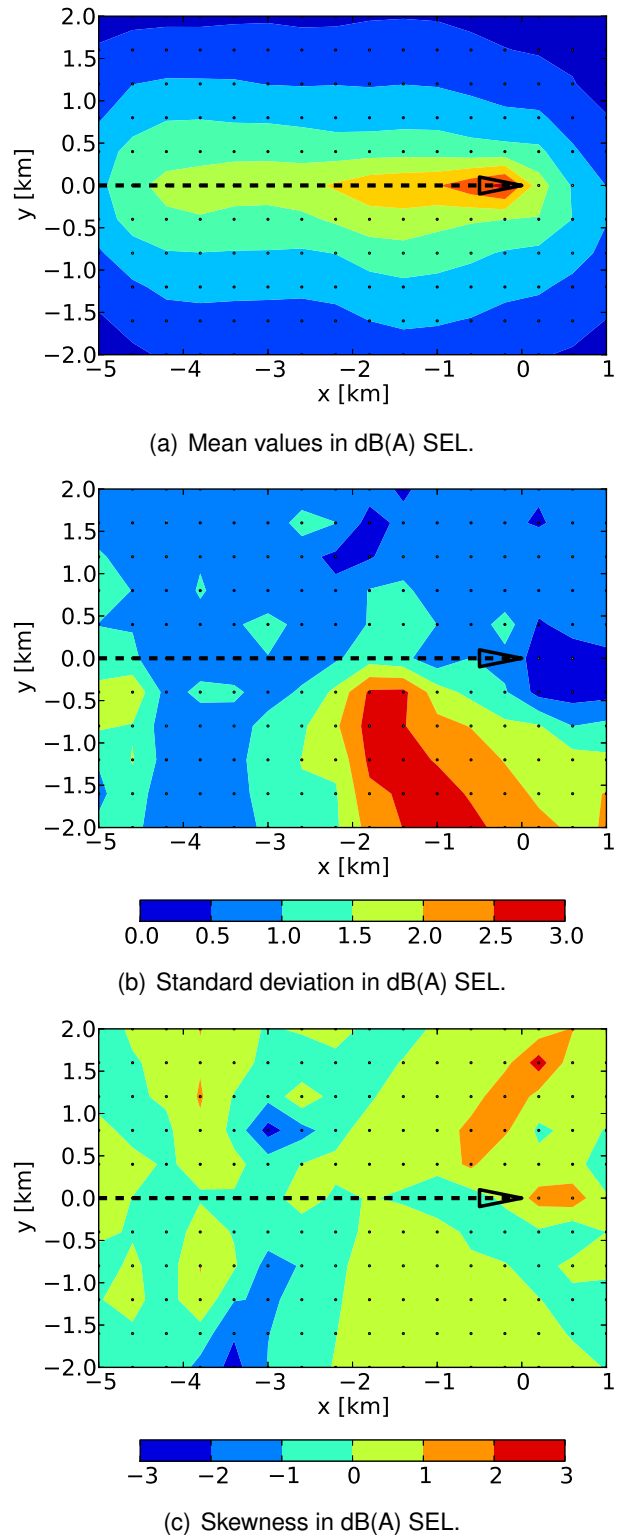


Figure 6: Mean, standard deviation and skewness computed by using a 7th order PCE with the  $y$  and  $z$  position and the magnitude of the velocity at the third control point as uncertain parameters.

to the observer. In SELENE the effect of wind on the sound propagation through the atmosphere is taken into account by a ray tracing method<sup>8</sup>.

In the presence of wind a choice needs to be made to prescribe the procedure based on air-speed or ground speed. Here it is chosen to use a prescribed ground speed. For this investigation the same procedure as presented in the previous section is used. However, the velocity at the start of the procedure is lowered from 100 knots to 86 knots, in order not to exceed the maximum air-speed of the helicopter. Landings are usually performed with a head wind component. According to the EC135 flight manual Category A take-off and landing procedures with a tail wind component are prohibited, therefore a head wind will be assumed.

The influence of uncertainty in the wind magnitude is investigated first. The stability of the atmosphere is chosen as “III/1-III/2-neutral”, as described in<sup>8</sup>. A Beta distribution with  $\alpha = 2$  and  $\beta = 2$  is chosen for the wind magnitude. The minimum and maximum values (10 m above ground level) are set to 0 and 5 m/s, respectively. The mean is 2.5 m/s and the standard deviation is 0.94 m/s.

In a previous section the velocity magnitude at only one control points was considered, which changes the acceleration along the flight path significantly. Note that here the wind has influence on the entire flight path. The acceleration will still be affected by the wind magnitude since the wind magnitude is dependent on height, however, its effect is less than when varying the velocity directly at one control point.

The results of the computation are shown in figure 7. In the figures the wind is blowing from right to left. The appearance of an acoustic shadow zone is clearly observed on the right in figure 7(a). Since the location of this shadow zone depends on the wind velocity large values of the standard deviation can be expected near the edge of the shadow zone. This is clearly seen in the plot of the standard deviation in figure 7(b). Inside the shadow zone the statistical values do not make sense since the noise level is theoretically  $-\infty$  dB in this region. Outside of the shadow zone the effect of wind is comparable to that of the velocity investigated in the previous section. However, the region where the standard deviation is

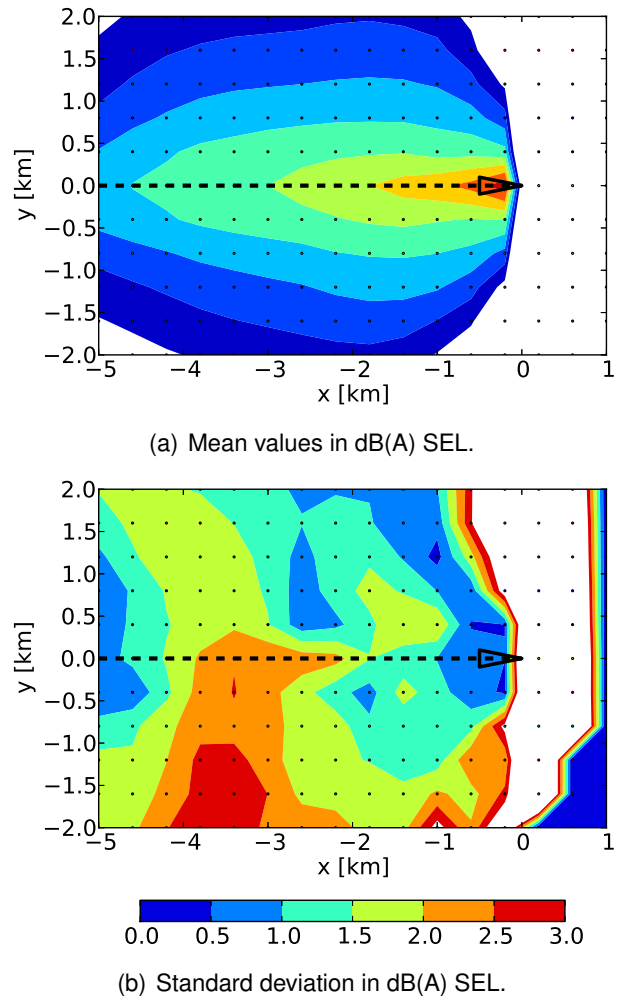
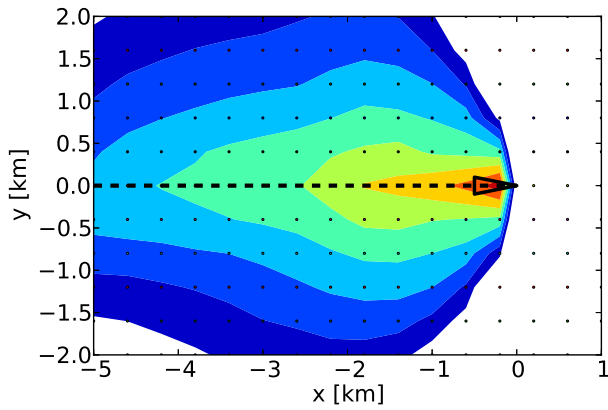


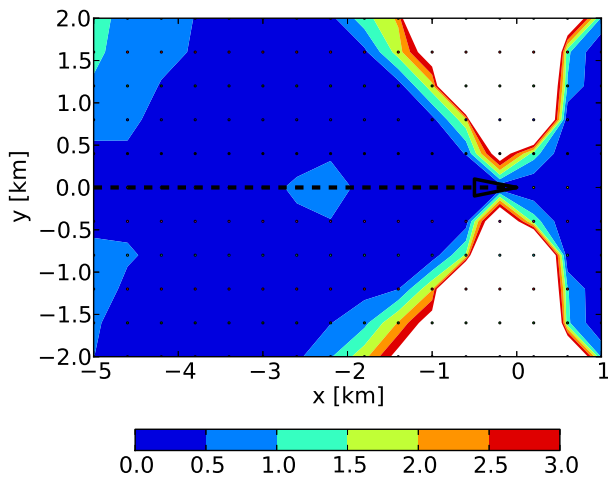
Figure 7: Mean and standard deviation of the SEL noise footprint due to uncertain wind magnitude. Results obtained by a 7th order PCE.

maximal is shifted to the left but is again on the advancing blade side. This effect of wind magnitude uncertainty is not surprising since the velocity over ground is prescribed and the head wind component directly influences the airspeed of the helicopter. The skewness is not shown, since its interpretation is very difficult due to PDF's with multiple maxima, however, the values outside the shadow zone are comparable to those in figure 4(d).

Next the effect of uncertainty in wind direction is investigated. In this case the wind velocity at 10 meters above ground level is fixed at 3 m/s. For the wind direction a normal distribution is assumed with a mean in the head wind direction (which corresponds to a wind blowing in the negative  $x$ -direction) and a standard devia-



(a) Mean values in dB(A) SEL.



(b) Standard deviation in dB(A) SEL.

Figure 8: Mean and standard deviation of the SEL noise footprint due to uncertain wind direction.

tion of 10 degrees. As can be seen in figure 8(b) the standard deviation is very high at the locations where the edge of the shadow zone moves due to changes in wind direction (values outside of the scale are white). At other locations the standard deviation is less than 1 dB(A) SEL. The skewness, not shown, displays rather large values compared to those observed in the previous sections.

The investigation presented above indicates that variations in wind magnitude have a more significant influence on the statistical distribution of noise on the ground than variations in wind direction.

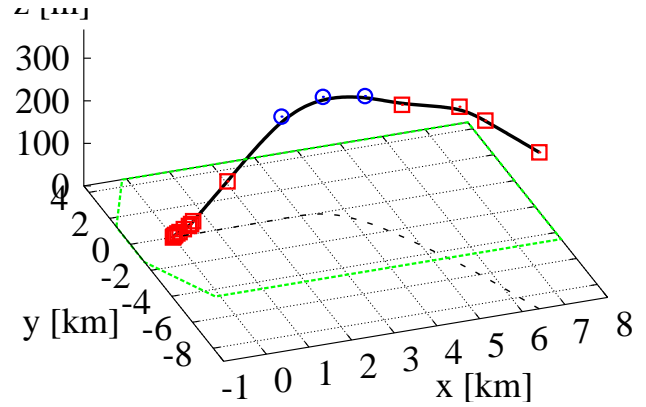


Figure 9: VFR reference approach flight path, with control points.

## 3.2 Three-dimensional procedures

In the previous sections the PCE method has been applied to a simple reference procedure. In this section the method is applied to more complex procedures. A reference procedure and a noise optimised procedure will be considered. Based on the results obtained in the previous sections it is chosen to only consider the magnitude of the velocity at three control points as uncertain parameters.

### 3.2.1 Reference procedure

The reference procedure reflects a standard approach procedure for an EC135 helicopter under Visual Flight Rules (VFR) at Braunschweig–Wolfsburg Airport. This procedure has been established with the help of the official visual operation chart of the airport, feedback from DLR test pilots and simulator tests.

The flight path is shown in figure 9. The landing point is located at  $(x, y, z) = (0, 0, 0)$ . The last part of the approach, from  $x = 3$  km to the landing point follows a 6 degrees descent. In the figures the markers are the control points of the spline that defines the flight path. The last part of the procedure contains many control points in order to model the flare and to meet the specifications at the landing decision point. The projection of the flight path on the horizontal plane is shown by the dashed line. The green line indicates the area covered by the microphones.

Since the number of uncertain variables should be kept low, three uncertain parameters are chosen for the investigation of the statistical prop-

id. #	Min.	Max.	$\mu$	$\sigma$	$\alpha$	$\beta$
5	48	62	55.7	3.8	1.3	1.05
6	45	60	53.5	3.1	2.65	2.0
7	30	52	41.9	3.1	5.3	3.6

Table 3: Parameters of the Beta distributions for the magnitude of the velocity at the 3 control points of the reference procedure. Velocity values in m/s.

erties of the reference procedure. The control points where the magnitudes of the velocity are considered as uncertain variables are shown in figure 9 by the blue circular markers. The red square markers are control points that are fixed. The magnitudes of the velocity are again modeled by beta distributions, whose parameters are given in table 3. The parameters of the distribution are chosen such that the mode of the distribution corresponds to the value of the undisturbed procedure. The identification number of the control point is given in the first column. The control point at the start of the procedure at  $(x, y, z) = (6400, -9000, 367)$  m has id. # 1.

The PCE is a 7th order expansion. In figure 10(a) the SEL footprint of the reference procedure is shown, in this case the procedure is flown exactly as specified (no uncertainties). In this figure the solid black line indicates the contour that was used for the optimisation, discussed in more detail in the next section. The difference between the contour levels is 5 dB(A). Figure 10(b) shows the mean SEL footprint of the reference procedure, with the same contour levels as in figure 10(a) and the solid black line corresponds to the same contour value. The mean SEL footprint displays an increase in noise compared to the footprint of the undisturbed approach. This could be due to the unsymmetric distribution of the velocity. To illustrate the difference between the footprint of the undisturbed procedure and the mean footprint a difference plot is shown in figure 10(c). Here positive values indicate that the mean value is above that of the undisturbed footprint value. The standard deviation is shown in figure 10(d). Here standard deviations of up to 2 dB(A) can be observed and the largest values occur below the flight path or on the advancing blade side.

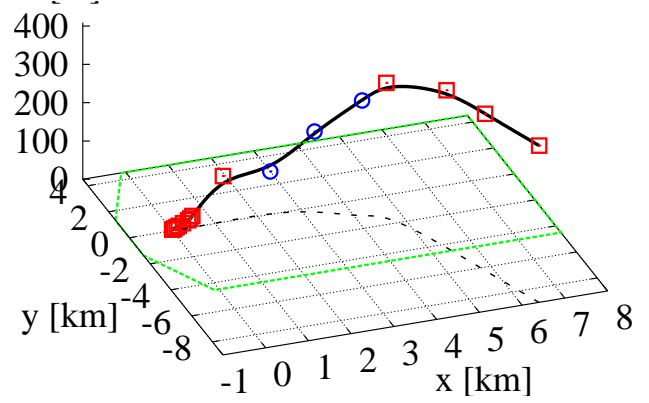


Figure 11: Noise optimized VFR approach flight path with control points.

### 3.2.2 Noise optimized procedure

In the previous section the reference procedure was presented. For the same scenario a noise optimized procedure has been developed. The procedure was optimised in order to minimize the area inside a given SEL contour. This contour is shown in figure 10(a) by the solid black line. The flight path of this optimised procedure is shown in figure 11. The flight path in the horizontal plane looks very similar to that of the reference procedure, shown in figure 9. The path in the vertical plane looks, however, different. The initial height at the start of the procedure is increased with respect to the reference procedure and the descent starts earlier.

As with the reference procedure the magnitudes of the velocity at three control points are considered as uncertain parameters. The parameters of the Beta distributions of the magnitude of the velocity of the optimized procedure are given in table 4. Again the parameters of the distributions are chosen such that the mode of the distribution corresponds to the value of the undisturbed procedure.

id. #	Min.	Max.	$\mu$	$\sigma$	$\alpha$	$\beta$
4	48	62	55.7	3.8	1.3	1.05
5	45	62	53.9	3.6	2.9	2.35
6	38	54	46.4	3.1	2.9	2.59

Table 4: Parameters of the Beta distributions for the magnitude of the velocity at the 3 control points of the noise optimized procedure. Velocity values in m/s.

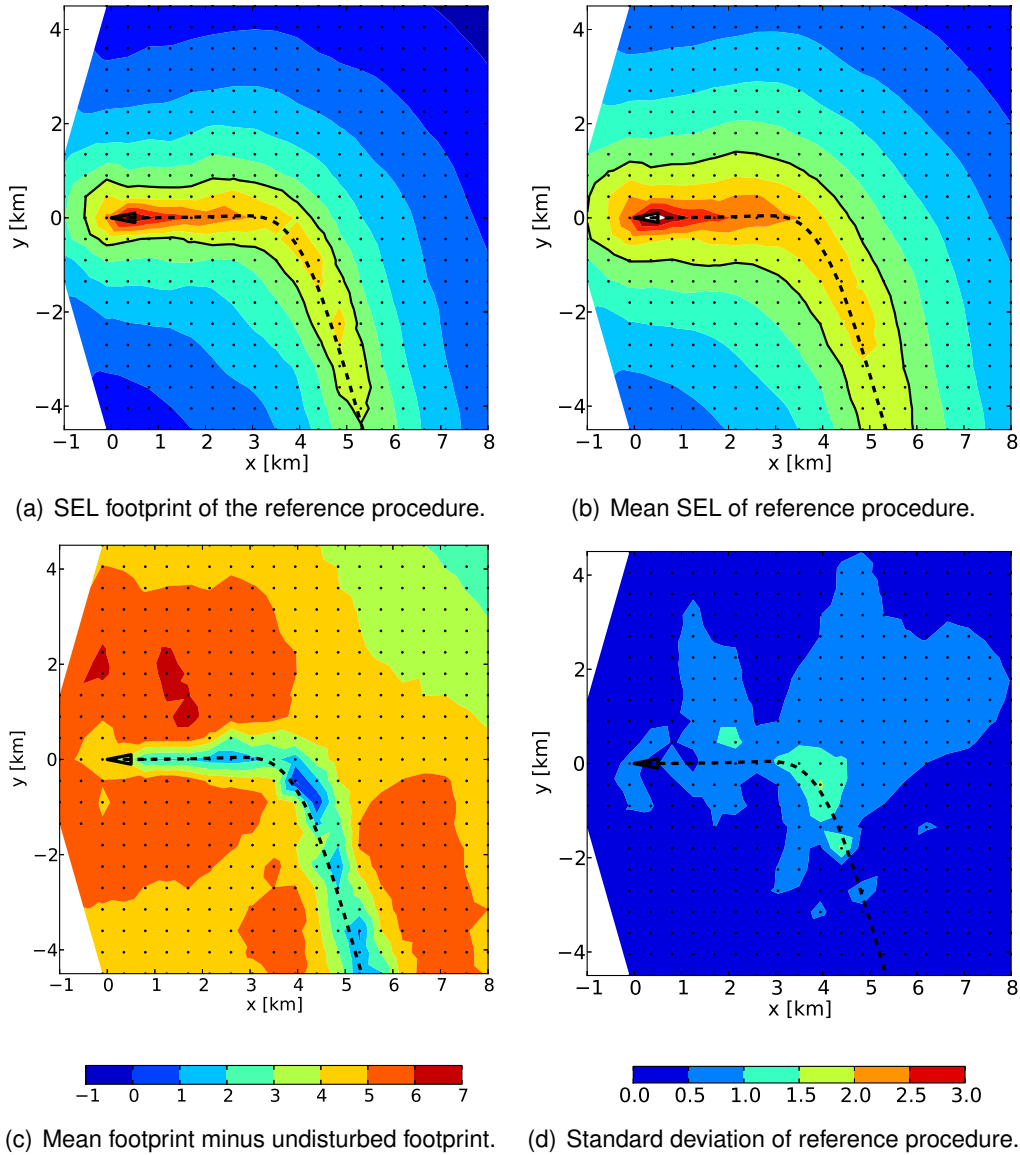


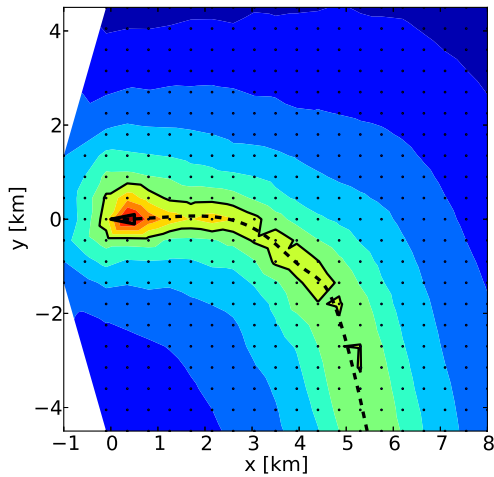
Figure 10: SEL footprint of the reference procedure with mean value and standard deviation obtained by a 7th order PCE. Values in dB(A) SEL.

The results are obtained for a 7th order PCE. The SEL footprint of the undisturbed noise optimised procedure is shown in figure 12(a) with the same contour levels as in figure 10(a). A reduction of the area inside the black contour of 60% is obtained. The area for the optimised procedure has become narrower and shorter. The mean footprint is shown in figure 12(b) and again displays higher levels compared to the footprint obtained for the undisturbed procedure. When the area's inside the mean SEL contours are compared (figure 10(b) and figure 12(b)) the reduction is only 17%. Note that the black contours of the mean value plots are not closed such that

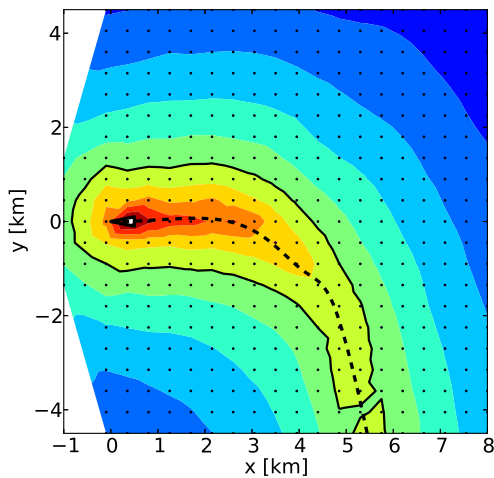
the comparison not fully reliable. The standard deviation of the optimised procedure, seen in figure 12(c), is larger compared to that observed for the reference procedure and displays value of up to 3 dB(A) SEL. This illustrates that it is important to consider uncertainty in the flight path in the optimisation.

## 4 CONCLUSIONS

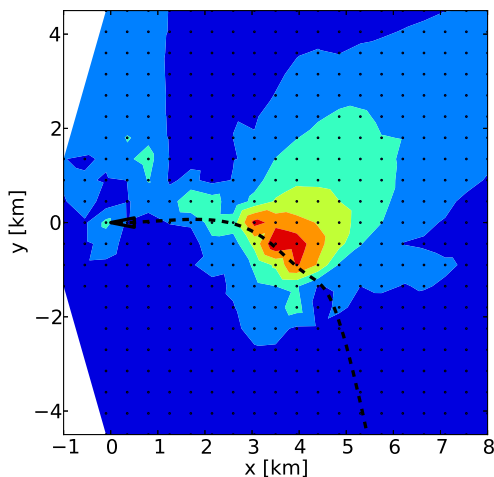
In this paper a method for uncertainty quantification of flight procedures has been investigated and applied. The method of polynomial chaos expansion has been used for this purpose.



(a) SEL footprint of optimized procedure.



(b) Mean SEL footprint of optimized procedure.



(c) Standard deviation of optimized procedure.

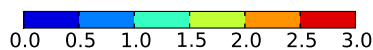


Figure 12: SEL footprint of the optimised procedure with mean value and standard deviation obtained by a 7th order PCE. Values in dB(A) SEL.

Initial computations for a simple two-dimensional approach procedure for the EC135 helicopter indicate that uncertainty in the velocity along the flight path has a more significant influence on the uncertainty in the sound exposure level noise footprint on the ground, compared to uncertainties in the position. The most plausible explanation for this is that the velocity has a strong influence on the acceleration, which directly influences the tip path plane angle of attack.

The same two-dimensional approach procedure was used to investigate the influence of wind magnitude and direction. For this purpose the ray tracing module implemented in the computational chain SELENE was used. It can be concluded that uncertainty in the wind magnitude has more influence on the sound exposure level noise footprint than uncertainty in the wind direction.

Application of the uncertain quantification to more complex three-dimensional procedures, with uncertainty in the velocity, shows that the mean value in general displays higher noise levels as compared to the undisturbed procedures. This could be due to the typical unsymmetric probability distribution of the velocity. Furthermore a significant increase in the standard deviation of the sound exposure levels on the ground is observed for the optimised procedure. The computations indicate that it would be useful to take the uncertainty of design parameters into account in the optimization process. However, the choice of the cost function for such an optimisation is not trivial. One would like to minimize the mean noise level at every microphone location and at the same time minimise the standard deviation of the noise level distribution at the microphone locations. If this succeeds a robust flight procedure with minimal noise is obtained. However, this is a multiobjective optimization problem which quickly becomes an intractable problem as there are many microphone locations.

The uncertainty quantification presented in this paper yields results that can be used to compare different procedures in terms of robustness (standard deviation). But the process could also be used to derive requirements/specifications for a flight guidance system in order to achieve a prescribed statistical distribution of the noise on the ground.

## ACKNOWLEDGMENTS

The research leading to these results has received funding from the European Community's Seventh Framework Programme (FP7/2007-2013) for the Clean Sky Joint Technology Initiative under grant agreement n° CSJU-GAM-GRC-2008-001.

## REFERENCES

- [1] B. Adams, W. Bohnhoff, K. Dalbey, J. Eddy, M. Eldred, D. Gay, K. Haskell, P. Hough, and L. Swiler. DAKOTA, A Multilevel Parallel Object-Oriented Framework for Design Optimization, Parameter Estimation, Uncertainty Quantification, and Sensitivity Analysis: Version 5.0 User's Manual. Technical Report SAND2010-2183, Sandia, 2009.
- [2] B. Benoit, A.-M. Dequin, K. Kampa, W. Von Grünhagen, P.-M. Basset, and B. Gimonet. HOST, a General Helicopter Simulation Tool for Germany and France. Virginia Beach, VA, USA, May 2-4 2000. American Helicopter Society 56th Annual Forum.
- [3] M. S. Eldred, C. G. Webster, and P. G. Constantine. Evaluation of Non-Intrusive Approaches for Wiener-Askey Generalized Polynomial Chaos. Schaumburg, IL, USA, April 2008. 49th AIAA/ASME/ASCE/AHS/ASC Structures, Structural Dynamics, and Materials Conference.
- [4] M. Gervais, V. Gareton, A. Dummel, and R. Heger. Validation of EC130 and EC135 environmental impact assessment using HELENA. Phoenix, AZ, USA, May 11-13 2010. Americal Helicopter Society 66th Annual Forum.
- [5] F. Guntzer, P. Spiegel, and M. Lummer. Genetic Optimization of EC-135 Noise Abatement Flight Procedures using an Aeroacoustic Database. Hamburg, Germany, September 22-25 2009. 35th European Rotorcraft Forum.
- [6] X. Li, P. Nair, Z. Zhang, L. Gao, and C. Gao. Aircraft robust trajectory optimization using nonintrusive polynomial chaos. *Journal of Aircraft*, 51:1592–1603, 2014.
- [7] W. F. J. Olsman and B. I. Gursky. Segment-wise measurement of helicopter approach noise with a reduced microphone setup. Montréal Canada, May 20-22 2014. Americal Helicopter Society 70th Annual Forum.
- [8] W. F. J. Olsman and M. Lummer. Influence of wind on the noise footprint of a helicopter landing. Amsterdam, The Netherlands, September 4-7 2012. 38th European Rotorcraft Forum.
- [9] R. Y. Rubinstein and D. P. Kroese. *Simulation and the Monte Carlo method*. John Wiley & Sons, Inc., second edition, 2008.
- [10] P. Spiegel, H. Buchholz, and M. Pott-Pollenske. Highly Instrumented BO105 and EC135-FHS Aeroacoustic Flight Tests including Maneuver Flights. Grapevine, TX, USA, June 1-3 2005. Americal Helicopter Society 61th Annual Forum.
- [11] N. Wiener. The homogeneous chaos. *Amer. J. Math.*, 60:897–936, 1938.
- [12] D. Xiu and G. E. Karniadakis. The Wiener-Askey Polynomial Chaos for Stochastic Differential Equations. *SIAM J. Sci. Comput.*, 24(2):619–644, Feb. 2002.

## COPYRIGHT STATEMENT

The authors confirm that they, and/or their company or organization, hold copyright on all of the original material included in this paper. The authors also confirm that they have obtained permission, from the copyright holder of any third party material included in this paper, to publish it as part of their paper. The authors confirm that they give permission, or have obtained permission from the copyright holder of this paper, for the publication and distribution of this paper as part of the ERF 2015 proceedings or as individual off-prints from the proceedings.